JOURNAL OF COMPUTATIONAL PHYSICS 43, 95–110 (1981)

Ion Extraction and Optics in 3D

J. W. WOOTEN

Computer Sciences Division, Oak Ridge National Laboratory, Oak Ridge, Tennessee 37830*

J. H. WHEALTON

Fusion Energy Division, Oak Ridge National Laboratory, Oak Ridge, Tennessee 37830*

D. H. MCCOLLOUGH AND R. W. MCGAFFEY

Computer Sciences Division, Oak Ridge National Laboratory, Oak Ridge, Tennessee 37830*

J. E. AKIN

University of Tennessee, Knoxville, Tennessee 37916

AND

L. J. DROOKS

Bell Laboratories, Whippany, New Jersey

Received December 16, 1980; revised April 27, 1981

An algorithm is described for a solution to the 3D Poisson Vlasov equations for ions extracted from a plasma. A variational formulation of Poisson's equation using isoparametric finite elements leads to a band matrix which is solved by a modified Gauss–Cholesky method. A semi-implicit method is described for the inclusion of nonlinear plasma electrons allowing an explicit solution of the extraction sheath. An intrinsically 3D example is shown.

I. INTRODUCTION

Ion beam extraction from a plasma is of interest in high energy neutral beam injectors for heating confined plasma. The optics of such ion beams have been

* Operated by Union Carbide Corporation under Contract W-7405-eng-26 with the U.S. Department of Energy.

0021-9991/81/090095–16$02.00/0

581/43/1-7

amenable to theoretical treatment in two dimensional cylindrical or slot geometries [1]. These 2D considerations have not been without influence on accelerator design [2, 3]. Nevertheless some intrinsically 3D phenomena need elucidation. Among these are cylindrical geometry beamlet steering by aperture displacement, beamlet–beamlet interaction, end effects in slots and transverse magnetic block direct-recovery devices.

Beamlet steering by aperture displacement in cylindrical geometry is susceptible to paraxial examination [4] thus relegating a 3D treatment to examining second order effects [5], with a qualitative examination of these second order effects available from a slot geometry calculation [3]. Inadvertent steering in cylindrical geometry by source plasma density variations is a 3D problem where no first order analysis is available, but qualitative information is again available for slot geometry. Beamlet–beamlet interaction in cylindrical geometry is also susceptible to a first order analysis [6] and slot qualitative analyses to all orders.

Slot end effects, however, do not fall into these categories since neither a paraxial analysis nor an alternate geometry configuration is claimed to represent the situation. In addition several important new lines of neutral beam generators are being constructed utilizing slots where the end effects are unknown. This is a principal reason for developing a 3D algorithm for ion beam optics. An alternative reason is to examine transverse magnetic blocking direct recovery experiments [7].

II. Physical Problem

The acceleration region of the neutral injector problem reduces to the simultaneous solution of two time-independent partial differential equations. One of these is Poisson's equation,

$$\nabla^2\phi = -\frac{e}{\varepsilon_0}(n_i - n_{e0}\exp[-e(\phi_0 - \phi)/kT_e]), \tag{1}$$

where

e is the electronic charge,

ε_0 is the permittivity of free space,

k is Boltzmann's constant,

T_e is the electron temperature,

ϕ_0 is the electric potential at the center of the source plasma,

n_{e0} is the electron number density at the center of the source plasma, and

n_i is the ion number density.

The other equation is Vlasov's equation,

$$\mathbf{v}\cdot\nabla f_i + \frac{q}{m}(-\nabla\phi)\cdot\frac{\partial f_i}{\partial \mathbf{v}} = 0, \tag{2}$$

where

q is the charge of an ion,

m is the mass of an ion, and

$f_i = f_i(\mathbf{r}, \mathbf{v})$ is the ion distribution function.

The two equations are connected by the ion density n_i, which is given by

$$n_i = \int d^3v f_i(\mathbf{r}, \mathbf{v}). \tag{3}$$

Direct solution of the Vlasov equation is, in general, extremely difficult, so we chose to solve it indirectly by an orbit-tracing technique.

The procedure used is almost identical to one used in a number of other attacks on the problem [8–10].

The solution steps are:

(1) With zero space charge (i.e., $n_i = n_{e0} = 0$), solve Eq. (1) in the region of interest.

(2) Using the potentials obtained, trace ion trajectories through the volume.

(3) Use the trajectory information to calculate the amount and distribution of space charge, n_i.

(4) The space charge obtained in (3), together wth the electron contribution ($n_{e0} e^{-e(\phi_0 - \phi)/kTe}$) becomes the inhomogeneous term for the new solution of Poisson's equation.

(5) Return to (2), and continue until the solution converges.

Due to the nonlinear form of Eq. (1), it is evident that an iterative procedure will be needed to find the solution. Equation (1) is rewritten using

$$\begin{aligned} u &= e(\phi_s - \phi)/kTe, \\ \eta_s &= e(\phi_0 - \phi_s)/kTe, \end{aligned} \tag{4}$$

where ϕ_s is the potential at the classical sheath edge as defined by Self [11] and η_s is the normalized potential drop between the center of the source plasma and the sheath edge.

Using these, we have, for Eq. (1),

$$\frac{\partial^2 u}{\partial x^2} + \frac{\partial^2 u}{\partial y^2} + \frac{\partial^2 u}{\partial z^2} = \left(\frac{n_i}{n_{e0}} - e^{-u} e^{-\eta_s} \right) \Big/ \lambda_D^2, \tag{5}$$

where $\lambda_D^2 = \varepsilon_0 kT_e/(n_{e0} e^2)$ is the electron Debye length in the center of the source plasma.

Let u in Eq. (5) be the value at the nth iteration, and u' be the value at iteration $n + 1$.

Then we have

$$\frac{\partial^2 u'}{\partial x^2}+\frac{\partial^2 u'}{\partial y^2}+\frac{\partial^2 u'}{\partial z^2}=\frac{1}{\lambda_D^2}\left(\frac{n_i}{n_{e0}}-e^{-u'}e^{-\eta_s}\right). \tag{6}$$

Now

$e^{-u'}$ can be expanded to first order in a Taylor series, viz.,

$$e^{-u'}=e^{-u}-e^{-u}\,du. \tag{7}$$

Approximating du by $(u'-u)$, we have

$$e^{-u'}=e^{-u}-e^{-u}(u'-u). \tag{8}$$

Then we may rewrite Eq. (8) as

$$e^{-u'}+u'e^{-u}=e^{-u}+ue^{-u}=e^{-u}(1+u). \tag{9}$$

Thus Eq. (6) becomes

$$\frac{\partial^2 u'}{\partial x^2}+\frac{\partial^2 u'}{\partial y^2}+\frac{\partial^2 u'}{\partial z^2}-\frac{e^{-u}e^{-\eta_s}}{\lambda_D^2}u'=\frac{1}{\lambda_D^2}\left(\frac{n_i}{n_{e0}}-e^{-u}e^{-\eta_s}(1+u)\right). \tag{10}$$

Note that the left-hand side (of Eq. (10)) includes both u and u', while the right-hand side contains only u. In this form, iterations may be performed until u' and u agree to within some error estimate.

III. Finite Element Solution of Nonlinear Poisson Equation

The boundary conditions for the three-dimensional problem can be somewhat formidable. To solve Eq. (10) in a general three-dimensional region, the finite element method was chosen [12].

The finite element method requires an integral statement of the problem. We introduce an approximate solution $\rho \simeq u$ and choose the method of weighted residuals. That is, define a residual error, R, due to the approximation

$$R=\nabla^2\rho'-\frac{e^{-\rho}e^{-\eta_s}\rho'}{\lambda_D^2}-\frac{1}{\lambda_D^2}\left(\frac{n_i}{n_{e0}}-e^{-\rho}e^{-\eta_s}(1+\rho)\right), \tag{11}$$

and require its weighted integral, I, to vanish,

$$I=\int_v WR\,dV=0. \tag{12}$$

For a Galerkin formulation, one assumes the weighting function to be $W = \rho'$, subject to the condition that the weights vanish on the boundary, so that,

$$I = \int_V \left[\nabla^2 \rho' - \frac{e^{-\rho} e^{-\eta_s}}{\lambda_D^2} \rho' - \frac{1}{\lambda_D^2} \left(\frac{n_i}{n_{e0}} - e^{-\rho} e^{-\eta_s} (1 + \rho) \right) \right] \rho' \, dV = 0. \tag{13}$$

Note that in Eq. (13) the first terms involving the Laplacian involve second derivatives and would involve C^1 continuity of the approximation just to calculate ρ'. This is undesirable. Noting that

$$\frac{\partial}{\partial x} \left(\rho \frac{\partial \rho}{\partial x} \right) = \left(\frac{\partial \rho}{\partial x} \right)^2 + \rho \frac{\partial^2 \rho}{\partial x^2}, \tag{14}$$

we use this in Eq. (13) to get

$$I = \int_V \left\{ - \left(\frac{\partial \rho'}{\partial x} \right)^2 - \left(\frac{\partial \rho'}{\partial y} \right)^2 - \left(\frac{\partial \rho'}{\partial z} \right)^2 - \frac{e^{-\rho} e^{-\eta_s} (\rho')^2}{\lambda_D^2} \right.$$
$$\left. - \frac{1}{\lambda_D^2} \left(\frac{n_i}{n_{e0}} - e^{-\rho} e^{-\eta_s} (1 + \rho) \right) \rho' \right\} dV + \int_S \rho' \left(\frac{\partial \rho'}{\partial n} \right) dS = 0. \tag{15}$$

Now since the weighting function was chosen to vanish on the boundaries and $\partial \rho' / \partial n$ will vanish on Neumann boundaries due to symmetries in the problem, we have no contribution to the solution from the integral over the surface.

Then we have,

$$\int_V \left\{ \left(\frac{\partial \rho'}{\partial x} \right)^2 + \left(\frac{\partial \rho'}{\partial y} \right)^2 + \left(\frac{\partial \rho'}{\partial z} \right)^2 + \frac{e^{-\rho} e^{-\eta_s}}{\lambda_D^2} (\rho')^2 \right\} dV$$
$$= \frac{1}{\lambda_D^2} \int_V \left\{ \frac{-n_i}{n_{e0}} + e^{-\rho} e^{-\eta_s} (1 + \rho) \right\} \rho' \, dV. \tag{16}$$

Introducing the standard finite element procedure, assume that the total integral is the sum of the element integrals, i.e.,

$$I = \sum_{i=1}^{m} I_e. \tag{17}$$

With a typical element the dependent variable is approximated by interpolation equations of the form

$$\rho^e(x, y, z) = \overset{1 \times N}{[H(x, y, z)]} \overset{N \times 1}{\{\rho_e\}}, \tag{18}$$

where the $\{\rho^e\}$ are the N nodal values of ρ, and $[H^e]$ contains the N interpolation equations of the element. The integral formulation requires global derivatives such as

$\partial\rho/\partial x$, etc., Within a typical element this would be approximated by employing Eq. (18). That is,

$$\frac{\partial \rho^e}{\partial x} = \left[\frac{\partial H^e}{\partial x}\right] \{\rho^e\}, \qquad \text{etc.,} \tag{19}$$

so that all quantities are expressed in terms of the unknown nodal potentials, $\{\rho^e\}$.

Letting $[H]$ and $[H]_{,x}$ denote the matrix of interpolation functions and their x derivative, respectively, Eq. (16) for one element becomes

$$\int_{V_e} \{\rho'_e\}^T \left([H]_{,x}^T[H]_{,x} + [H]_{,y}^T[H]_{,y} + [H]_{,z}^T[H]_{,z} + \frac{e^{-\rho}e^{-\eta_s}}{\lambda_D^2}[H]^T[H]\right) \{\rho'_e\}\, dV_e$$

$$= \frac{1}{\lambda_D^2}\int_{V_e} \{\rho'\}^T \left(\frac{-n_i}{n_{e0}} + e^{-\rho}e^{-\eta_s}(1+\rho)\right) dV_e. \tag{20}$$

We may write this as

$$[S_e]\{\rho'_e\} = \{C_e\}, \tag{21}$$

where

$$[S_e] = \int_{V_e} \left([H]_{,x}^T[H]_{,x} + [H]_{,y}^T[H]_{,y} + [H]_{,z}^T[H]_{,z} + \frac{e^{-\rho}e^{-\eta_s}}{\lambda_D^2}[H]^T[H]\right) dV_e, \tag{21a}$$

$$\{C_e\} = \frac{1}{\lambda_D^2}\int_{V_e} [H]^T \left(\frac{-n_i}{n_{e0}} + e^{-\rho}e^{-\eta_s}(1+\rho)\right) dV_e, \tag{21b}$$

and $\{\rho'_e\}$ are the new element nodal values.

Now the solution over the total volume is given by (17) so that

$$[S] = \sum_{I=1}^{m} [S_e], \tag{22a}$$

$$\{C\} = \sum_{I=1}^{m} \{C_e\}, \tag{22b}$$

and

$$\{\rho'\} = \sum_{I=1}^{m} \{\rho'_e\}. \tag{22c}$$

This process of assembly is carried out by bookkeeping routines as in most finite element programs. Note that values for ρ from previous iterations can be obtained by interpolation from previous nodal values if so desired.

It is usual to perform the integrations in Eqs. (21a)–(21b) by quadratures in local coordinates [12], especially when isoparametric interpolation functions are chosen for the [H]'s in Eq. (18).

Since the partial derivatives are global derivatives, they must be converted to local derivatives, i.e.,

$$[\partial_g V] = [J]^{-1}\{\partial_e V\}, \tag{23}$$

where

$[\partial_g V]$ denotes the global derivative of a basis function,

$[\partial_e V]$ denotes the local derivative, and

$[J]^{-1}$ is the inverse of the Jacobian of the transformation from global to total variables.

Then $\int_{V_e} [H]_{,x}^T [H_{,x}]\, dV_e$ can be expressed approximately as

$$\sum_{i=1}^{NQP} W_i |J_i| \, [\partial_x H]_i^T [\partial_x H]_i \tag{24}$$

where

W_i are the tabulated quadrature weights,

$|J_i|$ is determinate of the Jacobian at the point i,

NQP = number of quadrature points, and

$[\partial_x H]_i$ are global derivatives of local basis functions at point i.

Now using (23),

$$[\partial_x H]_i = [J]^{-1}[\partial_e H]_i \tag{25}$$

we can evaluate the global derivatives in terms of local derivatives of the interpolation functions.

For polynomials of known order, NQP can be selected to evaluate the integral. The minimum allowable value of NQP is that which exactly integrates $|J|$.

Once the element contributions to the system square matrix $[S]$ in Eq. (21a) and the system column matrix $[C]$ in Eq. (21b) have been calculated and assembled as given by Eq. (22a) and (22b), the resulting band matrix can be factored using a modified Gauss–Cholesky algorithm. Back substitution using the column matrix $[C]$ yields the desired column matrix of solutions $\{\rho'\}$ (Eq. (22c)).

Since the procedure is iterative and because of the Taylor expansion for the electron term, this assembly and factorization must be done for each iteration of the electron term.

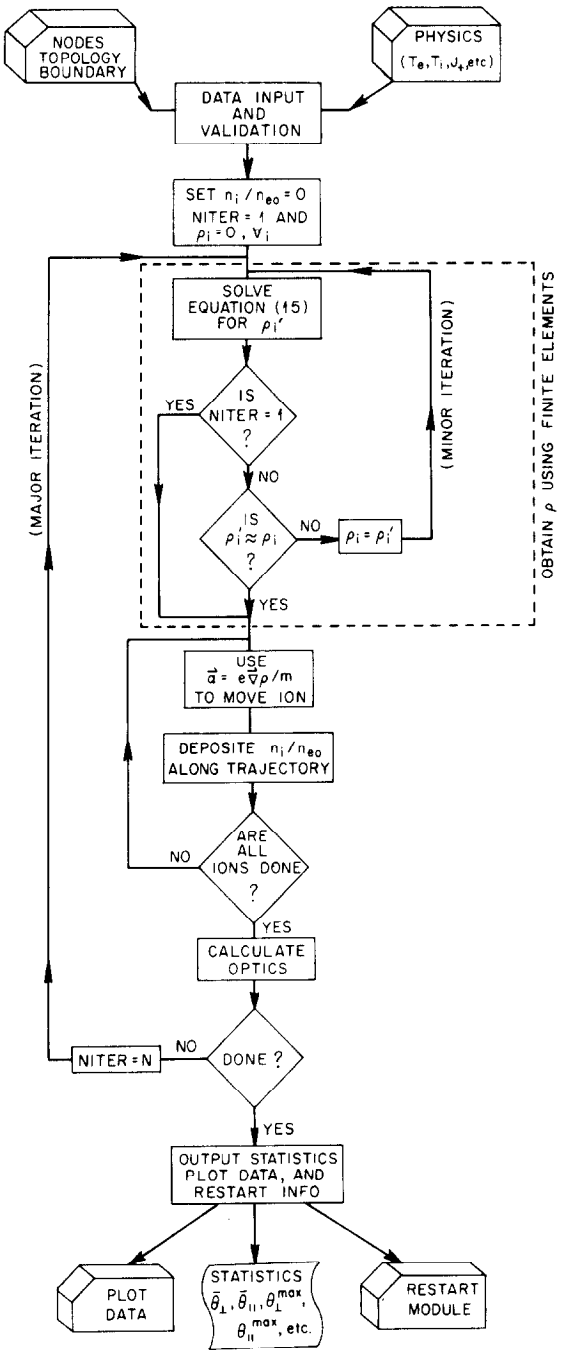

FIG. 1. Flowchart for 3D coupled Poisson–Vlasov code.

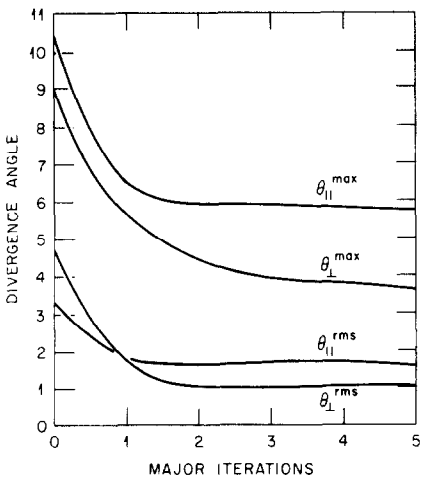

FIG. 2. Convergence of the root mean square and envelope divergence angles for a sample finite slot.

IV. VLASOV MODELING

After a set of potentials is found such that $u' \simeq u$, ions are propagated through the volume using

$$\mathbf{a} = -e\nabla\mathbf{u}/m, \tag{26}$$

where ∇u is determined using Eq. (23). The electric field produced by the potentials is assumed constant over a small volume $=\Delta x\Delta y\Delta z$.

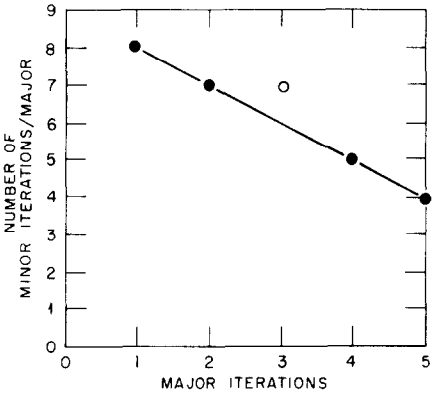

FIG. 3. Number of iterations of electron term required to converge nonlinear Poisson equation as a function of major ion iterations for the geometry illustrated in Fig. 6 (0 point was greatly over-converged).

Once the acceleration is known, the ions are moved along a parabolic path to a new location, $z' = z + \Delta z$. The charge carried by the ion is deposited at this location using the element interpolation functions [12] for use in the calculation of the potential upon completion of all ion trajectories.

The process of moving the ions through the electric fields is iterated on until we see optical convergence; that is, the optical properties of the beam remain stable over several iterations of charge-deposition and Poisson solution. Thus, the *major*

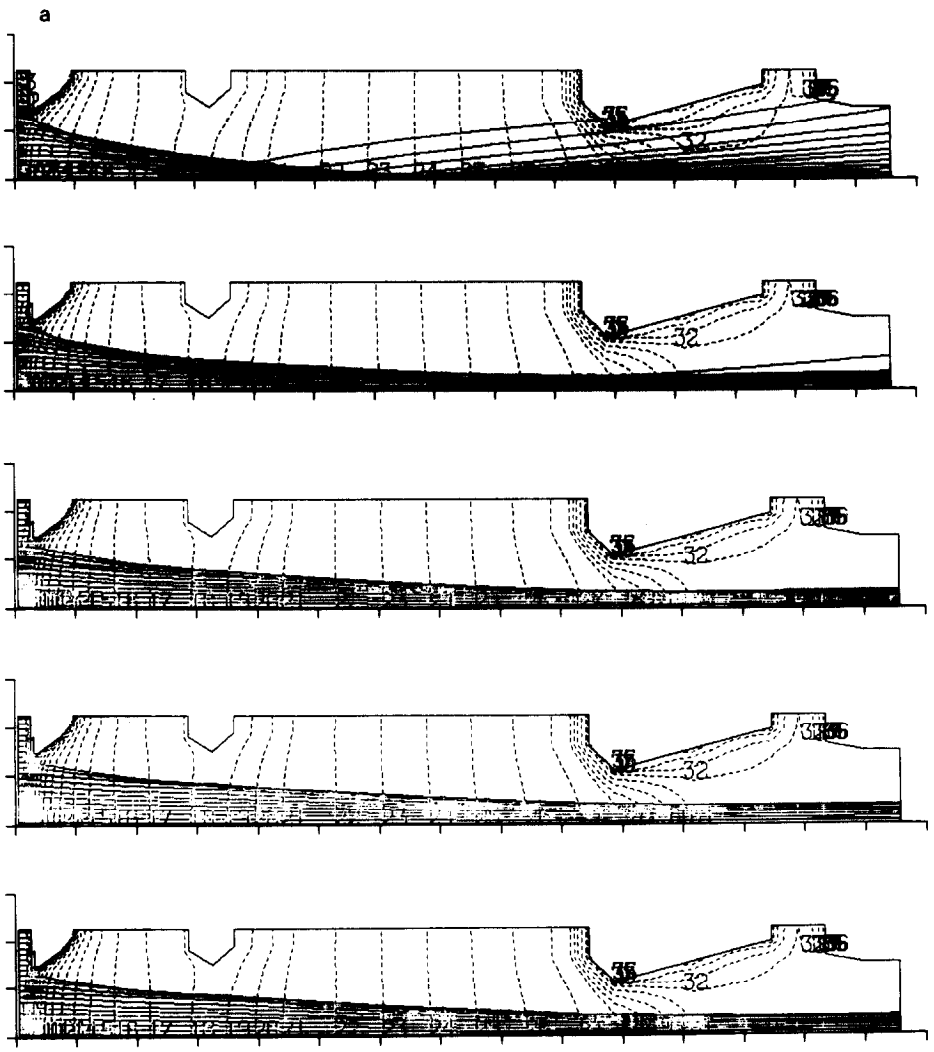

FIG. 4a. Side view of the central region of a finite slot solution (major iterations increase downward).

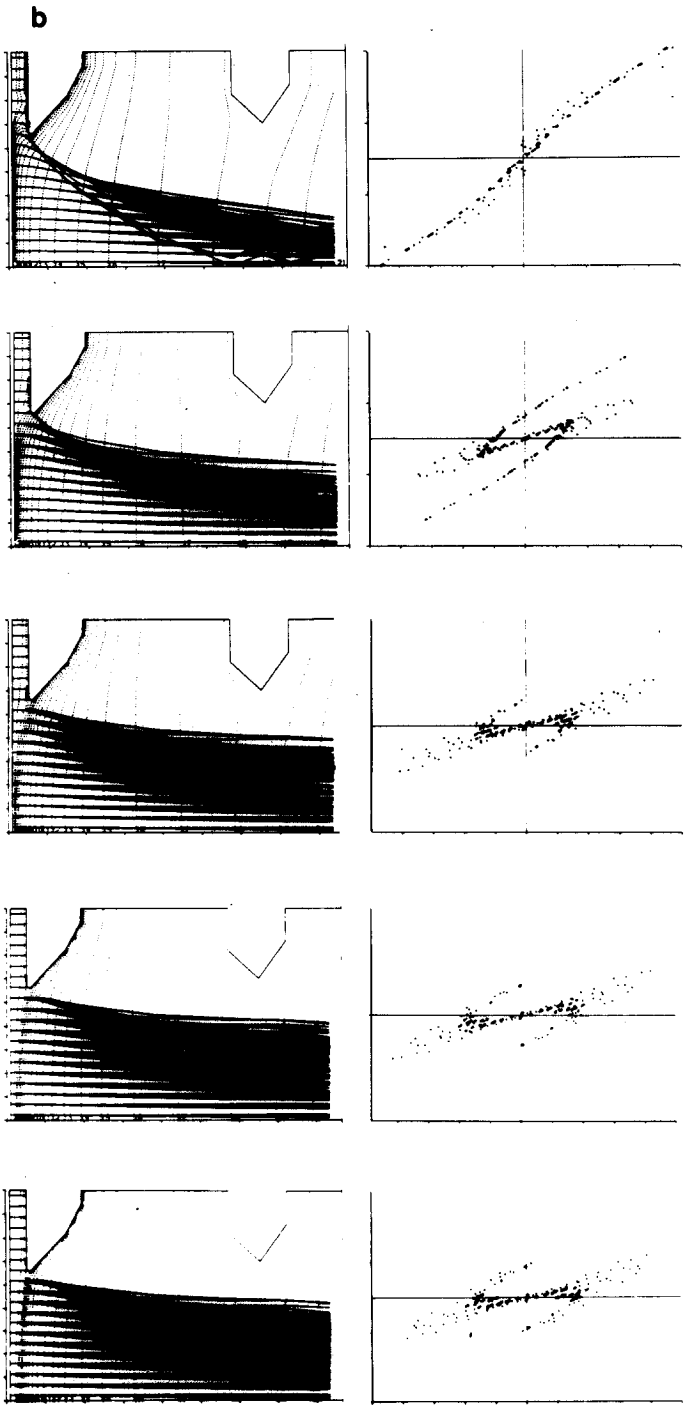

FIG. 4b. Side view of all orbits for a finite slot in region of plasma electrode with corresponding emittance diagrams (major iterations increase downward).

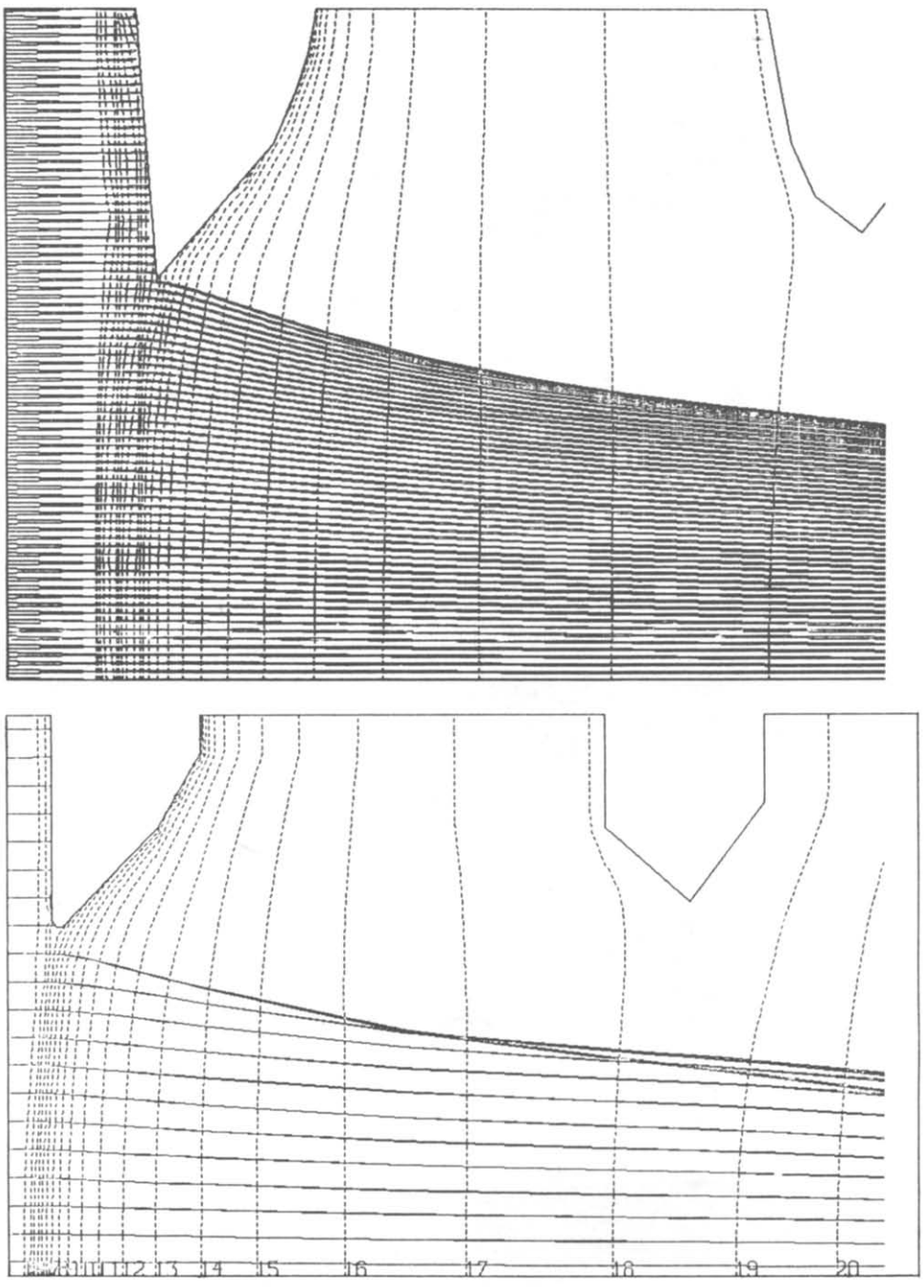

FIG. 5. A comparison in the extractor region of a 2D result (top) for an infinite slot with the 3D finite slot (bottom) at the symmetry plane.

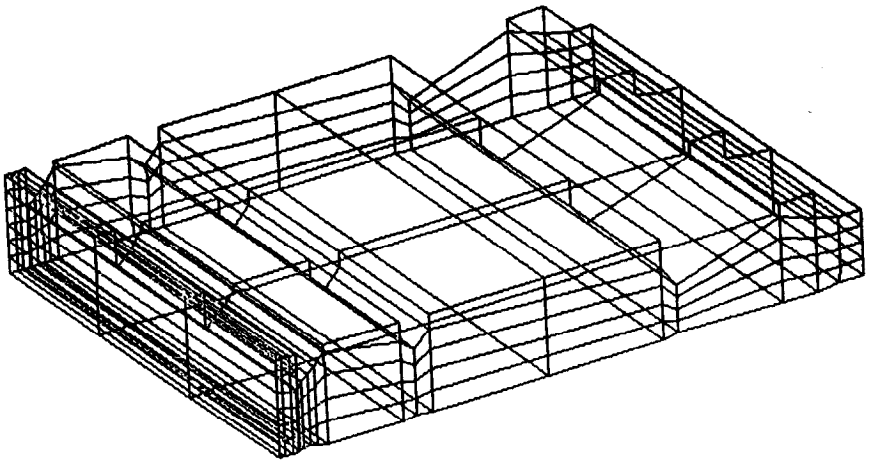

FIG. 6. The finite element mesh for the finite slot. The electrodes are on the top and the lower right-hand side.

iterations (or the ion tracing, charge deposition) are alternated with several *minor* iterations of solving Eq. (10) to obtain a consistent electric field for the new ion density function. A flow chart showing this procedure is shown in Fig. 1.

V. RESULTS

In Fig. 2 we show a plot of the root mean square beam divergence angle versus major iteration number for a three-dimensional solution of a finite slot. The computational effort done in solving each major iteration is characterized by the

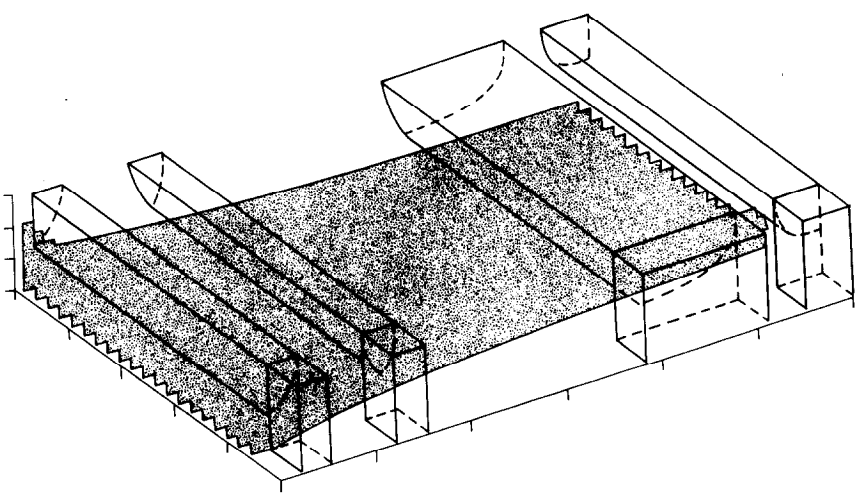

FIG. 7. Perspective view of all ion orbits with superimposed electrodes.

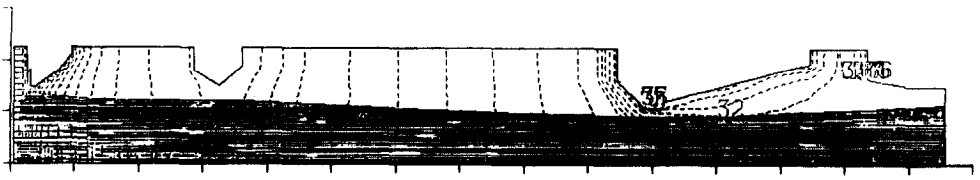

FIG. 8. Side view of all orbits in a finite slot. (Potentials are at symmetry plane.)

number of minor iterations per major iteration. A plot of the number of minor iterations against the major iterations is shown in Fig. 3. The number of minor iterations is a function of the convergence parameter for the potentials in Eq. (10). For this example, it was chosen such that good agreement with the 2D results described below would obtain.

In Fig. 4, we see the rapid formation of a stable sheath with significant details

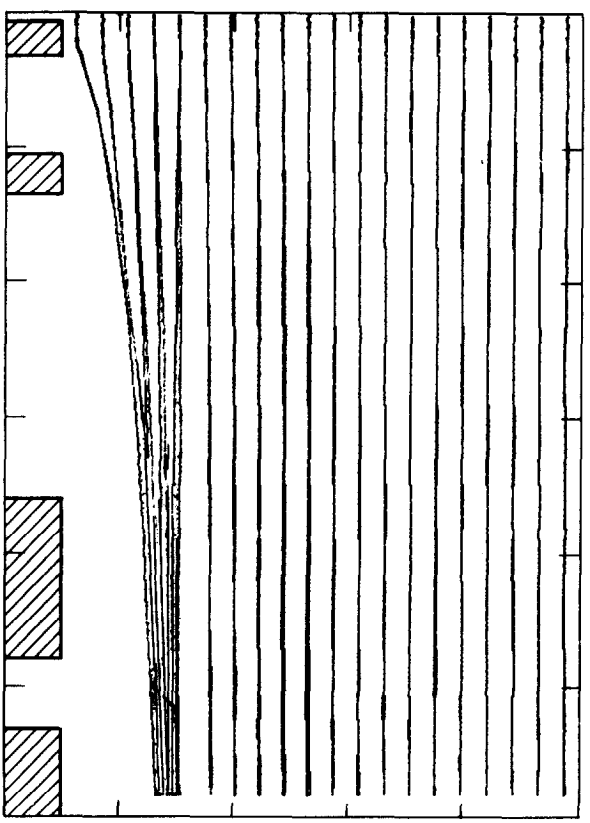

FIG. 9. Top view of all orbits in finite slot.

visible after only a few iterations. This is the first finite element explicit solution for the sheath in either two or three dimensions; there is one other explicit sheath solver, and that is a 2D finite difference algorithm [1]. Both of these algorithms converge for arbitrary perveance. Other ion extraction algorithms must use an emitting surface that is of the same dimensionality as their solution and is arbitrarily specified [8, 10].

The solution time for a given problem is greatly influenced by mesh size since the computational time for the Poisson solution goes as W^2, where W is the half bandwidth of the square matrix $[S]$. Also the orbit tracing time depends upon the number of cells traversed and the number of orbits run. Our present runs are made using 2433 nodal points, in 416 elements leading to a half bandwidth of 193 with 2433 system equations and 20 element degrees of freedom. During each major iteration, 400 ion orbits are traced through the device. The number of nodal points and trajectories required are determined by convergence tests and are limited by computer memory and CPU time. The parameters chosen were sufficient for reasonable agreement with the 2D work described below.

In Fig. 5 we show a comparison of a converged solution using the 2D finite difference code at ORNL versus the 3D on a LBL-TFTR infinite slot [13]. While these codes solve Eqs. (1), (2), and (3) in totally different fashions, we obtain good agreement in the 2D limit. In Fig. 6 we show the finite element mesh of a slot design with square ends. In Fig. 7 is a preliminary view of the orbits for a converged 3D solution with Fig. 8 giving a side view of the orbits through the device while Fig. 9 gives a top view. As can be seen in Figs. 7–9, the ends of the electrodes have an effect

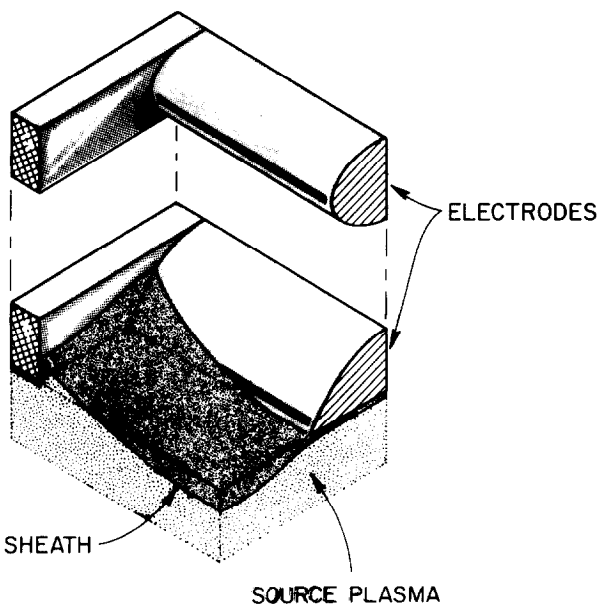

FIG. 10. Illustration of slot end near extraction electrode. Intrusion of sheath into corner produces 3D effects on divergence angles.

upon the ion beam. In Fig. 10, we show the plasma sheath at the first electrode, where the corner effects are clearer. A quantitative study of this effect as a function of several controlling variables is the subject of future work.

REFERENCES

1. J. H. WHEALTON *et al.*, *J. Comput. Phys.* **27** (1978), 333; J. C. WHITSON *et al.*, *J. Comput. Phys.* **28** (1978), 408; J. H. WHEALTON, *J. Comput. Phys.* **40** (1981), 491; J. H. WHEALTON, *Nucl. Instrum. Methods*, in press.
2. J. H. WHEALTON AND C. C. TSAI, *Rev. Sci. Instrum.* **49** (1978), 495; J. H. WHEALTON *et al.*, *Appl. Phys. Lett.* **33** (1978), 278; J. H. WHEALTON AND J. C. WHITSON, *Part. Accel.* **11** (1980), 14; J. H. WHEALTON *et al.*, *J. Appl. Phys.* **49** (1978), 3091; J. H. WHEALTON *et al.*, *J. Appl. Phys.*, in press; J. H. WHEALTON AND J. C. WHITSON, *J. Appl. Phys.* **50** (1979), 3964; J. H. WHEALTON *et al.*, *Nucl. Instrum. Methods* **154** (1978), 441; J. H. WHEALTON *et al.*, *Rev. Sci. Instrum.* **48** (1977), 829; L. R. GRISHAM *et al.*, *Rev. Sci. Instrum.* **48** (1977), 1037; J. KIM *et al.*, *J. Appl. Phys.* **49** (1978), 517.
3. J. H. WHEALTON *et al.*, *Appl. Phys. Lett.* **36** (1980), 91.
4. J. H. WHEALTON, *Rev. Sci. Instrum.* **48** (1977), 1428; W. L. GARDNER, J. KIM, M. M. MENON, AND J. H. WHEALTON, *Rev. Sci. Instrum.* **49** (1978), 1214.
5. L. J. DROOKS *et al.*, *Bull. Amer. Phys. Soc.* **23** (1978), 846; L. J. DROOKS *et al.*, Oak Ridge National Laboratory Report ORNL/TM-6740 (1979); J. W. WOOTEN *et al.*, *in* "Proceedings, Third International Symposium on Computer Methods for Partial Differential Equations," 1979.
6. J. H. WHEALTON, *Appl. Phys. Lett.* **33** (1978), 697; **32** (1978), 353.
7. H. H. HASELTON *et al.*, *in* "Proceedings, Sixth Symposium on Engineering Problems of Fusion Research," 1975; J. H. WHEALTON *et al.*, *Bull. Amer. Phys. Soc.* **25** (1980), 983; J. H. WHEALTON *et al.*, *Bull. Amer. Phys. Soc.* **25** (1980), 919.
8. K. HALBACH, LBL-444, "Mathematical Models and Algorithms for the Computer Program 'WOLF'," December 1975.
9. E. F. JAEGER AND J. C. WHITSON, ORNL/TM-4990, 1975, unpublished.
10. B. M. MARDER, Sand 77-0048, 1977, unpublished.
11. S. A. SELF, *Phys. Fluids* **6** (1963), 1762.
12. K. H. HUEBNER, "The Finite Element Method for Engineers," Wiley, New York, 1975; O. C. ZIENKIEWICZ, "The Finite Element Method in Engineering Science," McGraw–Hill, London, 1971.
13. K. H. BERKNER *et al.*, *in* "Proceedings, Seventh Symposium on Engineering Problems of Fusion Research," p. 1405, 1977, unpublished.